Inorganic Chemistry

Article

pubs.acs.org/IC

Salen-Based Coordination Polymers of Iron and the Rare Earth Elements

Asamanjoy Bhunia, Yanhua Lan, Valeriu Mereacre, Michael T. Gamer, Annie K. Powell,* and Peter W. Roesky*

Institut für Anorganische Chemie, Karlsruher Institut für Technologie (KIT), Engesserstrasse 15, 76131 Karlsruhe, Germany

Supporting Information

ABSTRACT: Reaction of *N,N′*-bis(4-carboxysalicylidene)-ethylenediamine (H_4L) with iron(III) chloride and lanthanide nitrates resulted in the coordination polymers of composition $\{[Ln_2(FeLCl)_2(NO_3)_2(DMF)_5]\cdot(DMF)_4\}_n$ (Ln = Y, Eu, Gd, Tb, Dy). The polymers consist of iron-salen-based moieties having carboxylate linkers connected to rare earth atoms in a 1D chain structure. Thus, the iron-salen complex acts as a "metalloligand". Because of the twisting of the chains, porous structures are formed and possess large free void space. The magnetic studies of selected compounds exhibit weak intramolecular antiferromagnetic interactions of Ln−Ln. At 3, 30, and 80 K, the Mössbauer spectra of the iron−dysprosium compound show a strongly asymmetric quadrupole doublet with isomer shift and quadrupole splitting values typical for Fe^{III} ions in high spin state. In addition, an anomalous temperature dependence of both isomer shift and quadrupole splitting has been observed.

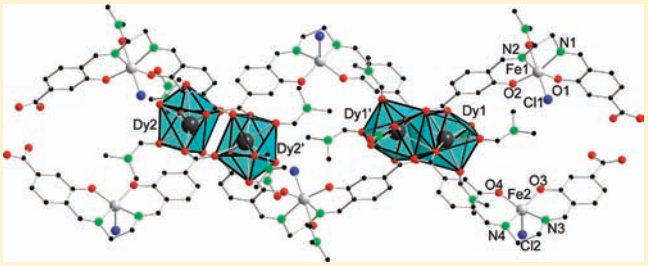

INTRODUCTION

Since the early work of Robson[1,2] on net-based coordination polymers around 1990[3,4] and the concept of reticular design initiated by Yaghi et al.[5,6] in the late 1990s, metal−organic frameworks (MOFs) and infinite coordination polymers (ICPs) have attracted the attention of a huge number of researchers.[2,7−10] Besides the fascinating structures based on a broad variety of molecular-based topologies there are promising applications[11] such as the storage of gases,[12,13] catalysis,[14] and sensors for special classes of molecules.[12,15] Some of these materials also show interesting physical properties such as magnetism,[16,17] luminescence,[18,19] and optoelectronic effects.[20] The synthesis of MOFs requires two main components: metal ions or metal ion clusters and rigid bi- or multifunctional organic linkers. The rigid bi- or multifunctional organic linkers sometimes referred to as "struts" serve to bridge the metal centers, which act as nodes and impose specified connectivities within the resulting MOF architecture.[9] The combination of a metal center and a linker has been designated as secondary building unit (SBU). By using this concept the MOF architecture can be easily analyzed.[21] Although mostly 3d metals have been used as metal centers,[9] some rare earth element based MOFs have also been reported.[10,22−27] In contrast to 3d metals the coordination numbers of the rare earth elements are higher and coordination geometries are hard to control.[23,26] On the other hand rare earth element based MOFs have shown interesting luminescent and magnetic properties.[27]

Whereas in most MOF materials rigid organic molecules are used as linkers, there are also some examples of "metalloligands" (MLs) in the literature.[8,13,14,28−31] In this approach, functionalized ligands (L) coordinate to a metal center (M) forming a "metalloligand" (ML) which is suitable for the construction of higher dimensional homo- or heterometallic ICPs or MOFs through the reaction with further metal centers. Kitagawa and co-workers reported microporous coordination polymers with unsaturated metal centers using ML systems.[32,33] The assembly of coordination polymers is a two step process: (1) synthesis of ML by the reaction of well-defined ligands and metal ions (mainly 3d metal ions) that together act as a linker (M1) and (2) reaction of ML with another metal ion (M2), which acts as a nodal unit in a framework.[32,33] In this context, some ICPs and MOFs consisting of salen (*N,N′*-bis-(salicylidene)ethylenediamine) based "metalloligands" with additional functional groups,[34] such as carboxylates,[32,35] pyridyl groups,[36] and benzoic acid groups[37] in para position to the OH group, have been reported.

Recently we reported on the salen ligand *N,N′*-bis(4-carboxysalicylidene)ethylenediamine (H_4L),[38] in which carboxylate groups are attached at meta positions to the OH groups.[39] As a result of the different stereochemistry compared to the established systems we expected a significant influence on the resulting structures of the coordination polymers. We found that in the presence of base, the metal functionalized two-dimensional coordination polymers $[Na_4(LM)_2\cdot(H_2O)_9]_n$ (M = Ni, Cu) were obtained.[39] We then introduced the salen-nickel complex as "metalloligand" in rare earth element-based MOFs.

Received: August 22, 2011
Published: November 14, 2011

Table 1. Crystallographic Details of 2−6

	1	2	3
chemical formula	$C_{51}H_{59}Cl_2Fe_2N_{11}O_{23}Y_2{\cdot}4(C_3H_7NO)$	$C_{51}H_{59}Cl_2Eu_2Fe_2N_{11}O_{23}{\cdot}4(C_3H_7NO)$	$C_{51}H_{59}Cl_2Fe_2Gd_2N_{11}O_{23}{\cdot}4(C_3H_7NO)$
formula mass	1846.90	1973.00	1983.58
crystal system	triclinic	triclinic	triclinic
a/Å	13.430(3)	13.616(3)	13.614(3)
b/Å	14.799(3)	14.823(3)	14.830(3)
c/Å	21.553(4)	21.566(4)	21.566(4)
α/deg	87.39(3)	87.36(3)	87.37(3)
β/deg	74.19(3)	74.43(3)	74.37(3)
γ/deg	77.21(3)	76.62(3)	76.58(3)
unit cell volume/Å^3	4018.9(14)	4078.5(14)	4078.0(14)
temperature/K	150(2)	200(2)	200(2)
space group	$P\bar{1}$	$P\bar{1}$	$P\bar{1}$
no. of formula units per unit cell, Z	2	2	2
radiation type	Mo$K\alpha$	Mo$K\alpha$	Mo$K\alpha$
absorption coefficient, μ/mm^{-1}	1.935	2.015	2.103
no. of reflections measured	42870	48395	42702
no. of independent reflections	21161	21451	21638
R_{int}	0.1309	0.0593	0.0809
final R_1 values ($I > 2\sigma(I)$)	0.0869	0.0430	0.0505
final $R_w(F^2)$ values (all data)	0.2457	0.1055	0.1321
goodness of fit on F^2	0.930	0.932	0.947

	4	5
chemical formula	$C_{51}H_{59}Cl_2Fe_2N_{11}O_{23}Tb_2{\cdot}4(C_3H_7NO)$	$C_{51}H_{59}Cl_2Dy_2Fe_2N_{11}O_{23}{\cdot}4(C_3H_7NO)$
formula mass	1986.92	1994.08
crystal system	triclinic	triclinic
a/Å	13.603(3)	13.582(3)
b/Å	14.829(3)	14.723(3)
c/Å	21.588(4)	21.432(4)
α/deg	87.40(3)	87.03(3)
β/deg	74.33(3)	74.25(3)
γ/deg	76.73(3)	76.10(3)
unit cell volume/Å^3	4080.3(14)	4003.7(14)
temperature/K	200(2)	150(2)
space group	$P\bar{1}$	$P\bar{1}$
no. of formula units per unit cell, Z	2	2
radiation type	Mo$K\alpha$	Mo$K\alpha$
absorption coefficient, μ/mm^{-1}	2.210	2.352
no. of reflections measured	57316	32415
no. of independent reflections	17298	14243
R_{int}	0.0695	0.1392
final R_1 values ($I > 2\sigma(I)$)	0.0401	0.0678
final $R_w(F^2)$ values (all data)	0.1059	0.1768
goodness of fit on F^2	1.019	0.999

By using this strategy we obtained the polymeric rare earth element-nickel compounds $\{[Ln_2(LNi)_3(DMF)(H_2O)_3]\cdot(DMF)_4\cdot(H_2O)_{10}\}_n$ (Ln = Er, Lu) and $\{[Dy(LNi)(DMSO)(NO_3)]\cdot(H_2O)_2\cdot(DMSO)\}_n$.[40] These compounds have unique structures, in which the salen-nickel unit acts as a flexible strut. Magnetic susceptibility measurements under zero dc field showed that the nickel−dysprosium compound exhibits a frequency dependence of out-of-phase components below 12 K indicating slow relaxation of its magnetization under these conditions. On the basis of these results we desire to extend our studies on other 3d−4f metal combination to study their magnetic properties. Herein we now report on salen based iron and rare earth element coordination polymers.

EXPERIMENTAL SECTION

General. IR spectra were obtained on a Bruker FTIR Tensor 37 Spectrometer via the Attenuated Total Reflection method (ATR). Elemental analyses were carried out with an Elementar vario EL Vario Micro Cube instrument TGA measurements were made on a Netzsch STA 429 instrument. *N,N′*-Bis(4-carboxysalicylidene)ethylenediamine (H_4L) was prepared according to literature procedures.[38] All other chemicals were used as purchased from commercial sources without further purification.

General Procedure for the Synthesis of Complexes 1−5. H_4L (39 mg, 0.11 mmol), $FeCl_3\cdot(H_2O)_6$ (27 mg, 0.1 mmol), $Ln(NO_3)_3\cdot(H_2O)_m$ (0.20 mmol), and pyridine (0.1 mL) were combined in 3 mL of DMF while stirring. The resulting solution was then stirred for another 3 h at room temperature and then sealed in a 10 mL glass vial. The glass vial was heated at 90 °C for 2d in oven and cooled to room temperature. The red block shaped crystals were

Scheme 1. Structures of Compound 1−5 Simplified for Clarity, for Example, No DMF is Shown

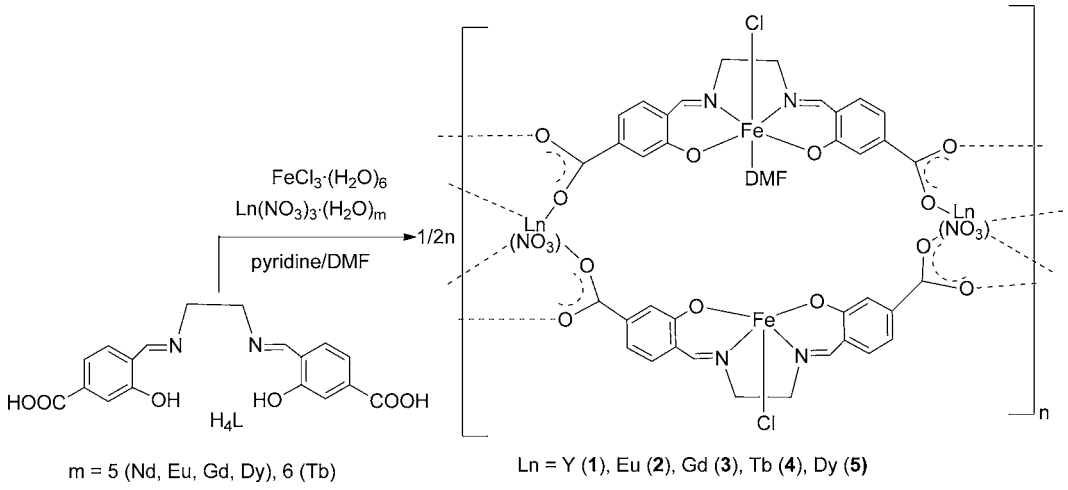

collected and washed three times with DMF followed by diethyl ether and dried in air.

{[Y$_2$(FeLCl)$_2$(NO$_3$)$_2$(DMF)$_5$]·(DMF)$_4$}$_n$ ***(1)***. Yield: 45 mg, 23% (based on Fe). IR [cm^{-1}]: ν = 2929 (w), 2855 (w), 1614 (s), 1531 (m), 1476 (m) (ν_1), 1403 (m), 1382 (m), 1307 (w), 1278 (m) (ν_2), 1196 (m), 1104 (m), 1046 (m) (ν_3), 976 (s), 903 (m), 814 (m) (ν_4), 801 (m), 776 (s), 741 (m), 678 (m), 631 (m), 534 (w), 496 (w), 413 (w). Anal. Calcd for $C_{63}H_{87}Cl_2Fe_2N_{15}O_{27}Y_2$: C, 40.97; H, 4.75; N, 11.38. Found: 40.18; H, 4.61; N, 10.41.

{[Eu$_2$(FeLCl)$_2$(NO$_3$)$_2$(DMF)$_5$]·(DMF)$_4$}$_n$ ***(2)***. Yield: 53 mg, 27% (based on Fe). IR [cm^{-1}]: ν = 2931 (w), 2862 (w), 1634 (m), 1613 (s), 1597 (m), 1532 (m), 1462 (m), 1435 (m) (ν_1), 1401 (w), 1384 (w), 1331 (m), 1305 (m), 1281 (m), 1253 (m) (ν_2), 1194 (w), 1107 (m), 1093 (m), 1061 (s), 1036 (m) (ν_3), 978 (m), 899 (w), 816 (m) (ν_4), 806 (w), 778 (m), 740 (s), 676 (m), 627 (w), 612 (m), 553 (w). Anal. Calcd for $C_{63}H_{87}Cl_2Eu_2Fe_2N_{15}O_{27}$: C, 38.35; H, 4.44 N, 10.65. Found: C, 37.83; H, 4.40; N, 10.27.

{[Gd$_2$(FeLCl)$_2$(NO$_3$)$_2$(DMF)$_5$]·(DMF)$_4$}$_n$ ***(3)***. Yield: 58 mg, 28% (based on Fe). IR [cm^{-1}]: ν = 2933 (w), 2914 (w), 1674 (m), 1647 (s), 1600 (s), 1531 (m), 1477 (m) (ν_1), 1401 (m), 1331 (m), 1301 (w), 1281 (s) (ν_2), 1253 (m), 1197 (m), 1107 (m), 1033 (m) (ν_3), 976 (s), 903 (w), 839 (m) (ν_4), 811 (m), 800 (w), 776 (s), 740 (s), 675 (s), 629 (m), 526 (w). Anal. Calcd for $C_{48}H_{52}Cl_2Fe_2Gd_2N_{10}O_{22}$ (corresponds to loss of the five DMF molecules): C, 35.63; H, 3.24; N, 8.66. Found: C 35.10; H, 3.34; N, 8.32.

{[Tb$_2$(FeLCl)$_2$(NO$_3$)$_2$(DMF)$_5$]·(DMF)$_4$}$_n$ ***(4)***. Yield: 56 mg, 28% (based on Fe). IR [cm^{-1}]: ν = 2933 (w), 2914 (w), 1671 (m), 1644 (s), 1600 (s), 1532 (m), 1464 (m) (ν_1), 1402 (s), 1384 (m), 1307 (m), 1282 (w), 1253 (m) (ν_2), 1194 (m), 1107 (m), 1093 (s), 1039 (s) (ν_3), 978 (m), 913 (w), 838 (m) (ν_4), 815 (m), 798 (s), 778 (m), 741 (s), 676 (s), 660 (w), 627 (s), 554 (w). Anal. Calcd for $C_{63}H_{87}Cl_2Fe_2N_{15}O_{27}Tb_2$: C, 38.08; H, 4.41 N, 10.57. Found: C, 37.63; H, 4.36; N, 10.01.

{[Dy$_2$(FeLCl)$_2$(NO$_3$)$_2$(DMF)$_5$]·(DMF)$_4$}$_n$ ***(5)***. Yield: 62 mg, 31% (based on Fe). IR [cm^{-1}]: ν = 2925 (w), 2860 (w), 1616 (s), 1532 (w), 1475 (m) (ν_1), 1404 (s), 1281 (s), 1253 (m) (ν_2), 1198 (m), 1104 (m), 1038 (m) (ν_3), 978 (s), 906 (w), 802 (m) (ν_1), 776 (s), 740 (s), 676 (s), 629 (s), 555 (w). Anal. Calcd for $C_{45}H_{45}Cl_2Dy_2Fe_2N_9O_{21}$ (corresponds to loss of the six DMF molecules): C, 34.75; H, 2.92 N, 8.10. Found: C, 34.63; H, 3.42; N, 8.20.

X-ray Crystallographic Studies of 1−5. A suitable crystal was covered in mineral oil (Aldrich) and mounted on a glass fiber. The crystal was transferred directly to the −73 °C or −123 °C cold stream of a STOE IPDS II diffractometer.

All structures were solved using the program SHELXS-97.[41] The remaining non-hydrogen atoms were located from successive difference in Fourier map calculations. The refinements were carried out by using full-matrix least-squares techniques on F^2, minimizing the function $(F_o - F_c)^2$, where the weight is defined as $4F_o^2/2(F_o^2)$ and F_o and F_c are the observed and calculated structure factor amplitudes using the program SHELXL-97.[41] The hydrogen atom contributions were calculated, but not refined. The final values of refinement parameters are given in Table 1. The locations of the largest peaks in the final difference Fourier map calculation as well as the magnitude of the residual electron densities in each case were of no chemical significance. Positional parameters, thermal parameters, bond distances, and angles have been deposited as Supporting Information.

Magnetic Measurements. The magnetic measurements were carried out with the use of a Quantum Design SQUID magnetometer MPMS7. This magnetometer works between 1.8 and 400 K for dc applied fields ranging from −7 to 7 T. Measurements were performed on the polycrystalline samples. The magnetic data were corrected for the sample holder and the diamagnetic contribution estimated from Pascal constants.

Mössbauer Spectroscopy. The Mössbauer spectra were acquired by using a conventional spectrometer in the constant-acceleration mode equipped with a ^{57}Co source (3.7 GBq) in rhodium matrix. Isomer shifts are given relative to α-Fe at room temperature. The polycrystalline sample was inserted in an Oxford Instruments Mössbauer-Spectromag 4000 Cryostat. The sample temperature can be varied between 3 and 300 K. Spectra were fitted by using the Normos Mössbauer Fitting Program.[42]

RESULTS AND DISCUSSION

Synthesis and Structures. The reaction of H_4L, $FeCl_3·(H_2O)_6$, and $Ln(NO_3)_3·(H_2O)_m$ (m = 5 (Eu, Gd, Dy), 6 (Y, Tb)) in the presence of DMF/pyridine under elevated temperature resulted in coordination polymers of composition $\{[Ln_2(FeLCl)_2(NO_3)_2(DMF)_5]·(DMF)_4\}_n$ (Ln = Y (**1**), Eu (**2**), Gd (**3**), Tb (**4**), Dy (**5**)) (Scheme 1).

All compounds were obtained as red crystalline materials and characterized by standard analytical and spectroscopic techniques. In the IR spectra, the antisymmetric and symmetric stretching bands for carboxylate groups are observed at around 1614 and 1403 cm^{-1} (**1**), 1597 and 1401 cm^{-1} (**2**), 1600 and 1402 cm^{-1} (**3**), 1611 and 1385 cm^{-1} (**4**), and 1616 and 1404 cm^{-1} (**5**).[43−45] The differences between antisymmetric and symmetric stretching bands indicate that the carboxylate group coordinated to the metal ions in a bridging fashion. The absence of a characteristic absorption band in the range of 1700 cm^{-1} indicates the complete deprotonation[43−45] of the salen ligands and coordination to metal ions. Moreover, the characteristic stretching vibrations bands (ν_1−ν_4) of the nitrate

dx.doi.org/10.1021/ic2018264 | Inorg. Chem. 2011, 50, 12697−12704

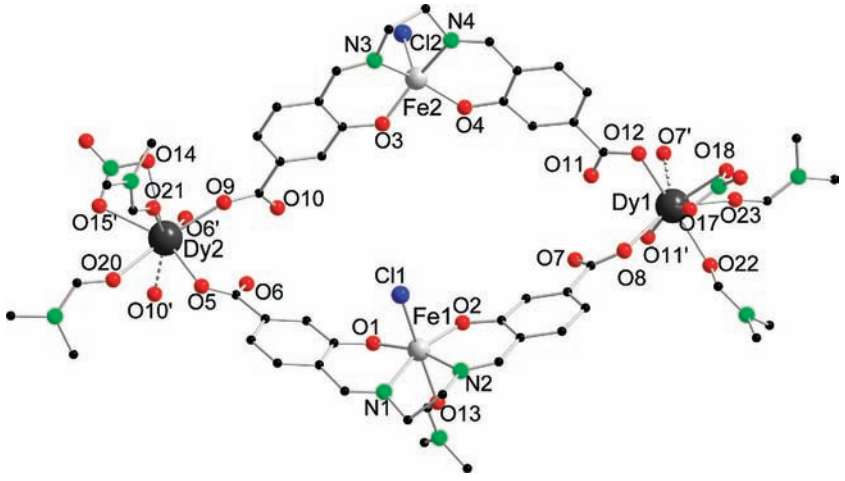

Figure 1. Solid state structures of compound **5**, shown is the coordination arrangement of a dysprosium dimer, omitting hydrogen atoms. Compounds **1**−**4** are isostructrual. Selected bond lengths [Å] and bond angles [deg]. **1**: Fe1−N1 2.115(6), Fe1−N2 2.113(5), Fe1−O1 1.906(5), Fe1−O2 1.895(4), Fe1−O13 2.144(6), Fe1−Cl1 2.365(2), Fe2−Cl2 2.226(3), Y1−O7 2.260(5), Y1−O8 ′2.311(5), Y1−O11′ 2.263(5), Y1−O12 2.374(5), Y1−O17 2.548(6), Y1−O18 2.451(6), Y1−O22 2.288(6), Y1−O23 2.420(5), Y2−O5 2.333(4), Y2−O6′ 2.265(5), Y2−O9 2.266(4), Y2−O10′ 2.327(5), Y2−O14 2.583(5), Y2−O15 2.427(5), Y2−O20 2.374(5), Y2−O21 2.338(6), N1−Fe1−N2 77.4(2), N1−Fe1−O1 89.4(2), N1−Fe1−O2 164.3(2), N1−Fe1−Cl1 90.32(2), N2−Fe1−O13 84.80(2), O1−Fe1−O13 84.7(2), O1−Fe1−Cl1 96.8(2), O13−Fe1−Cl1 174.89(15), N3−Fe2−Cl2 97.7(2), O3−Fe2−Cl2 111.6(2), O7−Y1−O8′ 129.8(2), O7−Y1−O11 65.9(2), O7−Y1−O11′ 76.4(2), O7−Y1−O12 75.4(2), O7−Y1−O17 133.2(2), O7−Y1−O18 91.2(2), O7−Y1−O22 140.3(2), O7−Y1−O23 72.5(2), O11′−Y1-O12 125.2(2), O17−Y1−O18 51.4(2), O22−Y1−O23 70.7(2), O5−Y2−O6′ 124.2(2), O6′−Y2-O9 77.3(2), O6′−Y2-O20 137.9(2), O6′−Y2-O21 138.9(2), O9−Y2−O10′ 130.1(2), O14−Y2−O15 50.3(2). **2**: Fe1−N1 2.119(3), Fe1−N2 2.127(4), Fe1−O1 1.906(3), Fe1−O2 1.909(3), Fe1−O13 2.167(3), Fe1−Cl1 2.366(15), Fe2−Cl2 2.232(2), Eu1−O7 2.328(3), Eu1−O8′ 2.385(3), Eu1−O11′ 2.347(3), Eu1−O12 2.427(3), Eu1−O17 2.590(4), Eu1−O18 2.509(4), Eu1−O22 2.347(3), Eu1−O23 2.483(3), Eu2−O5 2.400(3), Eu2−O6′ 2.340(3), Eu2−O9 2.314(3), Eu2−O10′ 2.386(3), Eu2−O14 2.619(4), Eu2−O15 2.493(3), Eu2−O20 2.429(3), Eu2−O21 2.409(4), N1−Fe1−N2 77.03(13), N1−Fe1−O1 87.64(13), N1−Fe1−O2 163.00(14), N1−Fe1−Cl1 93.30(10), N2−Fe1−O13 85.35(14), O1−Fe1−O13 90.81(14), O1−Fe1−Cl1 93.60(10), O13−Fe1−Cl1 174.89(11), N3−Fe2−Cl2 100.64(12), O3−Fe2−Cl2 105.42(13), O7−Eu1−O8′ 130.71(10), O7−Eu1−O11 66.07(9), O7−Eu1−O11′ 75.25(10), O7−Eu1−O12 74.86(10), O7−Eu1−O17 133.68(11), O7−Eu1−O18 94.03(13), O7−Eu1−O22 140.45(10), O7−Eu1−O23 72.41(11), O11′−Eu1-O12 124.90(10), O17−Eu1−O18 49.93(13), O22−Eu1−O23 71.38(12), O5−Eu2−O6′ 123.81(11), O6′−Eu2-O9 76.41(12), O6′−Eu2-O20 137.79(13), O6′−Eu2−O21 139.30(12), O9−Eu2−O10′ 130.94(11), O14−Eu2−O15 49.64(12). **3**: Fe1−N1 2.108(4), Fe1−N2 2.127(4), Fe1−O1 1.901(3), Fe1−O2 1.908(3), Fe1−O13 2.174(4), Fe1−Cl1 2.366(2), Fe2−Cl2 2.232(2), Gd1−O7 2.322(3), Gd1−O8′ 2.379(3), Gd1−O11′ 2.330(3), Gd1−O12 2.414(3), Gd1−O17 2.587(4), Gd1−O18 2.492(4), Gd1−O22 2.342(4), Gd1−O23 2.466(4), Gd2−O5 2.389(3), Gd2−O6′ 2.324(4), Gd2−O9 2.305(3), Gd2−O10′ 2.380(3), Gd2−O14 2.619(4), Gd2−O15 2.488(4), Gd2−O20 2.422(4), Gd2−O21 2.387(4), N1−Fe1−N2 77.31(14), N1−Fe1−O1 87.40(14), N1−Fe1−O2 162.92(15), N1−Fe1−Cl1 93.29(12), N2−Fe1−O13 84.8(12), O1−Fe1−O13 90.78 (15), O1−Fe1−Cl1 93.69(11), O13−Fe1−Cl1 174.80(12), N3−Fe2−Cl2 100.84(13), O3−Fe2−Cl2 105.60(14), O7−Gd1−O8′ 130.27(11), O7−Gd1−O11 65.54(11), O7−Gd1−O11′ 75.56(11), O7−Gd1−O12 74.70(12), O7−Gd1−O17 133.64(13), O7−Gd1−O18 93.95(14), O7−Gd1−O22 140.66(12), O7−Gd1−O23 72.47(12), O11′−Gd1-O12 124.97(11), O17−Gd1−O18 49.98(15), O22−Gd1−O23 71.49(13), O5−Gd2−O6′ 124.06(13), O6′−Gd2−O9 77.12(13), O6′−Gd2-O20 137.55(14), O6′−Gd2-O21 139.01(15), O9−Gd2−O10′ 130.62(12), O14−Gd2−O15 49.92(14). **4**: Fe1−N1 2.117(4), Fe1−N2 2.124(4), Fe1−O1 1.904(3), Fe1−O2 1.907(3), Fe1−O13 2.168(4), Fe1−Cl1 2.3669(16), Fe2−Cl2 2.232(2), Tb1−O7 2.305(3), Tb1−O8′ 2.353(3), Tb1−O11′ 2.308(3), Tb1−O12 2.402(3), Tb1−O17 2.571(4), Tb1−O18 2.480(4), Tb1−O22 2.322(3), Tb1−O23 2.460(3), Tb2−O5 2.367(3), Tb2−O6′ 2.303(3), Tb2−O9 2.290(3), Tb2−O10′ 2.368(3), Tb2−O14 2.608(4), Tb2−O15 2.467(4), Tb2−O20 2.393(4), Tb2−O21 2.371(4), N1−Fe1−N2 77.11(14), N1−Fe1−O1 87.53(13), N1−Fe1−O2 163.12(14), N1−Fe1−Cl1 93.26(11), N2−Fe1−O13 84.9(15), O1−Fe1−O13 90.61(14), O1−Fe1−Cl1 93.72(10), O13−Fe1−Cl1 174.88(11), N3−Fe2−Cl2 101.00(12), O3−Fe2−Cl2 105.78(14), O7−Tb1−O8′ 130.30(11), O7−Tb1−O11 65.81(10), O7−Tb1−O11′ 75.91(11), O7−Tb1−O12 75.11(11), O7−Tb1−O17 133.36(12), O7−Tb1−O18 92.96(14), O7−Tb1−O22 140.58(11), O7−Tb1−O23 72.34(11), O11′−Tb1-O12 125.22(11), O17−Tb1−O18 50.07(14), O22−Tb1−O23 71.41(12), O5−Tb2−O6′ 123.95(12), O6′−Tb2-O9 77.28(13), O6′−Tb2−O20 137.31(14), O6′−Tb2-O21 139.35(13), O9−Tb2−O10′ 130.29(11), O14−Tb2−O15 50.26(13). **5**: Fe1−N1 2.110(6), Fe1−N2 2.120(7), Fe1−O1 1.893(6), Fe1−O2 1.911(5), Fe1−O13 2.155(6), Fe1−Cl1 2.368(2), Fe2−Cl2 2.231(3), Dy1−O7 2.288(5), Dy1−O8′ 2.347(5), Dy1−O11′ 2.289(5), Dy1−O12 2.389(5), Dy1−O17 2.570(6), Dy1−O18 2.451(6), Dy1−O22 2.307(5), Dy1−O23 2.441(5), Dy2−O5 2.364(5), Dy2−O6′ 2.288(6), Dy2−O9 2.281(5), Dy2−O10′ 2.351(5), Dy2−O14 2.605(6), Dy2−O15 2.463(6), Dy2−O20 2.383(6), Dy2−O21 2.358(6), N1−Fe1−N2 77.0(3), N1−Fe1−O1 87.7(2), N1−Fe1−O2 163.4(3), N1−Fe1−Cl1 92.9(2), N2−Fe1−O13 85.5(2), O1−Fe1−O13 90.0(2), O1−Fe1−Cl1 93.9(2), O13−Fe1−Cl1 175.3(2), N3−Fe2−Cl2 100.3(2), O3−Fe2−Cl2 105.8(2), O7−Dy1−O8′ 129.7(2), O7−Dy1−O11 65.1(2), O7−Dy1−O11′ 76.0(2), O7−Dy1−O12 74.5(2), O7−Dy1−O17 133.7(2), O7−Dy1−O18 93.8(2), O7−Dy1−O22 141.1(2), O7−Dy1−O23 72.2(2), O11′−Dy1-O12 125.3(2), O17−Dy1−O18 50.8(2), O22−Dy1−O23 72.0(2), O5−Dy2−O6′ 123.4(2), O6′−Dy2−O9 77.2(2), O6′−Dy2-O20 137.2 (2), O6′−Dy2−O21 138.5(2), O9−Dy2−O10′ 129.3(2), O14−Dy2−O15 50.6(2).

group are observed (Experimental Section) in compounds **1**−**5**, and the difference in the wavenumber between ν_1 and ν_2 is about 200 cm^{-1}, indicating that the nitrate group coordinates to the metal ion in a bidentate chelating mode.[45] Because of the low solubility of all compounds no NMR data could be acquired.

The solid state structures were determined by single crystal X-ray diffraction (Figures 1 and 2). Compounds **1**−**5** crystallize in the triclinic space group $P\bar{1}$. They are isostructural to each other. Selected bond lengths and bond angles are listed in the caption of Figure 1. The asymmetric units of compounds **1**−**5** contain two rare earth ions (Ln1 and Ln2), two different Fe-

dx.doi.org/10.1021/ic2018264 | Inorg. Chem. 2011, 50, 12697−12704

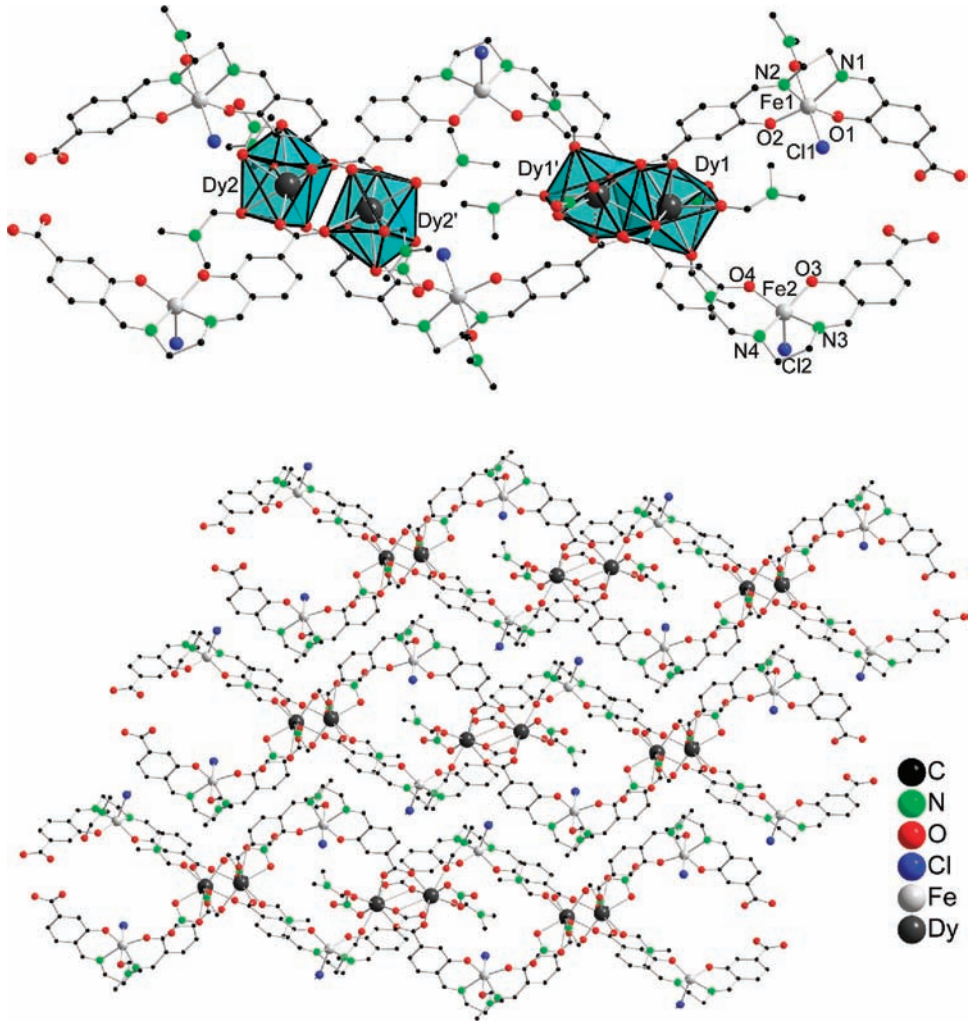

Figure 2. Solid-state structure of **5**, omitting hydrogen atoms. Top: The SBU is highlighted. Bottom: cutout of the polymeric structure. Compounds **1**−**4** are isostructrual.

salen units ((Fe1LCl1)(DMF)) and (Fe2LCl2)), two nitrate groups, five coordinating DMF molecules, and four non-coordinating DMF molecules. In the solid state structure two neighboring rare earth ions (Ln1, Ln1′ and Ln2, Ln2′) are connected together via four carboxylate groups from four different Fe-salen units (Figure 2, top). Both rare earth atoms form different secondary building units (SBUs).[10] One SBU, which is based on a $[(Ln)_2(\mu\text{-}O_2CR)_4(\eta^2\text{-}O_2NO)_2(DMF)_4]$ building block, is formed around Ln1 (Figure 2, top). This SBU can be regarded as a distorted square paddle-wheel built from two rare earth ions bridged by four carboxylates. Each Ln1 is 8-fold coordinated (Figure 1); they are ligated to four oxygen atoms of four metal bridging carboxylate groups from four different Fe-salen units (O7′, O8, O11′, and O12), one nitrate group (O17 and O18) and two molecules of DMF (O22 and O23). Two of the carboxylate groups are symmetrically coordinated between the metal centers whereas the other two carboxylate groups are asymmetrically bound. The coordination polyhedron of Ln1 can be best described as a distorted square antiprism. The other SBU is formed around Ln2. This SBU also consists of a $[(Ln)_2(\mu\text{-}O_2CR)_4(\eta^2\text{-}O_2NO)_2(DMF)_2]$ building block. The second SBU is a square paddle-wheel (Figure 2, top). Ln2 and Ln2′ are connected via four μ-bidantate carboxylate groups from four different Fe-salen units to form the paddlewheel unit (Figure 2, top). The SBU seen around Ln2 is comparable to the one around Ln1. Both SBUs are formed by two symmetrically and two asymmetrically coordinated carboxylate groups. The difference between the SBUs is found in the coordination of the asymmetrically bound unit. Ln2 is also ligated to eight oxygen atoms (Figure 1): four oxygen atoms (O5, O6′, O9, and O10′) from metal bridging carboylate groups of the Fe-salen unit, two oxygen atoms (O14 and O15) from one nitrate group and two oxygen atoms (O20 and O21) from two DMF molecules. This polyhedron can also be described as distorted square antiprism.

Since compounds **1**−**5** are isostructural, only the bonding parameters of compound **5** will be discussed in detail (Figures 1 and 2). The Dy−Dy distances in the paddlewheel units are 4.049(9) and 4.199(10) Å, respectively. The Dy−O bond distances are in the range of 2.281(5)−2.570(6) Å, which is comparable to reported dysprosium coordination polymers.[46−48] In the first Fe-salen unit ((Fe1LCl1)(DMF)), Fe1 is coordinated to the salen ligand, one chloride ion and one DMF molecule, resulting in a distorted octahedral geometry with the chloride ion and the oxygen atom of the DMF molecule in apical positions.[49] In the second Fe-salen unit (Fe2LCl2), Fe2 adopts a square-pyramidal geometry with a chloride ion in the apical position. The Fe−O and Fe−N bond

dx.doi.org/10.1021/ic2018264 | *Inorg. Chem.* 2011, 50, 12697−12704

lengths range from 1.873(5) Å to 2.155(6) Å and 2.078(6) Å to 2.120(7) Å, respectively, which is common for the Fe-salen unit.[50] The Fe−Cl bond distances in compound **5** are 2.368(2) Å and 2.231(3) Å for Fe1 and Fe2, respectively. Connecting the asymmetric units results in a 1D chain along the *a* axis having alternating paddlewheel units. Because of the twisting of the chains a porous structure is formed that possesses large free void space (Figure 2, bottom). The solvent DMF molecules occupy the void space. The total potential solvent accessible void volume of compound **5** calculated by PLATON is 28.3%.

Thermogravimetric Analysis (TGA). The TGA of compounds **1**−**5** are depicted in Figure 3. The TGA of

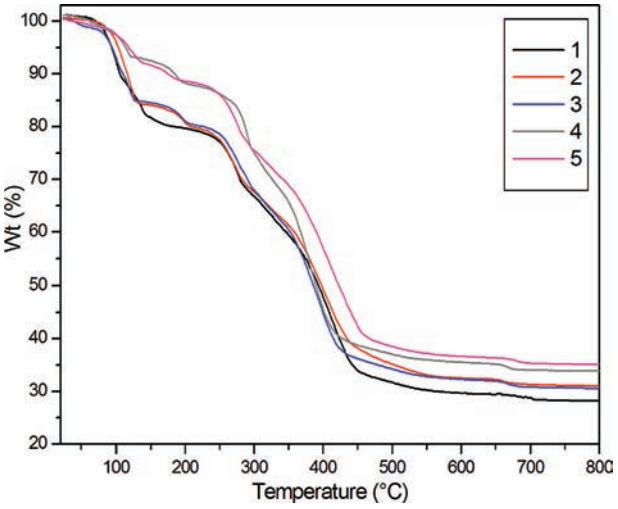

Figure 3. TGA curves for **1**−**5** in the temperature range of 20 to 800 °C at the heating rate of 5 °C/min under the N_2 atmosphere.

complex **1** shows that five DMF molecules are lost in the temperature range 70−180 °C (obsd 19.93%, calcd 19.79%). The remaining four DMF molecules are lost in the temperature range of 230−312 °C (obsd 14.94%, calcd 15.83%). The framework begins to decompose with a continuous weight loss up to 450 °C. Compound **2** shows a weight loss of 14.88% around 128 °C, corresponding to the release of four noncoordinated DMF molecules (calcd 14.82%); one coordinated DMF molecule is lost around 200 °C (obsd 4.31%, calcd 3.70%). The other four coordinated DMF molecules are released in the temperature range 240−310 °C. The TGA of compound **3** is similar to that of compound **2**: there is a weight loss in the temperature range 75−126 °C from the loss of four noncoordinated DMF molecules, a second weight loss arises in the temperature range 170−196 °C from the loss of one coordinated DMF molecule, and a weight loss in the temperature range 220−310 °C from the loss of four coordinated DMF molecules. The residues decompose after 450 °C. For **4**, the weight loss at 134 °C corresponds to the loss of two DMF molecules (obsd 6.78%, calcd 7.36%). Subsequently, five DMF molecules are lost in the temperature range 280− 342 °C (obsd 18.97%, calcd 18.39%). After loss of all lattice solvent molecules, the framework begins to decompose. For **5**, the weight loss at around 136 °C corresponds to the loss of two noncoordinated DMF molecules (obsd 7.92%, calcd 7.33%), followed by the release of two noncoordinated DMF molecules in the temperature range 160−260 °C (obsd 7.56%, calcd 7.33%). Additionally, a weight loss of 18.8% between 270−370 °C corresponds to the loss of five coordinated DMF molecules (calcd 18.33%). Finally, the framework begins to disintegrate with continuous weight loss after 450 °C.

Magnetic Properties of Compounds 3−5. Variable-temperature dc magnetic susceptibilities of compounds **3**−**5** were measured on polycrystalline samples. Under an applied dc field of 1000 Oe, the room temperature χT products of **3**−**5** are 25.30, 33.06, and 37.67 cm^3K/mol, respectively (Figure 4).

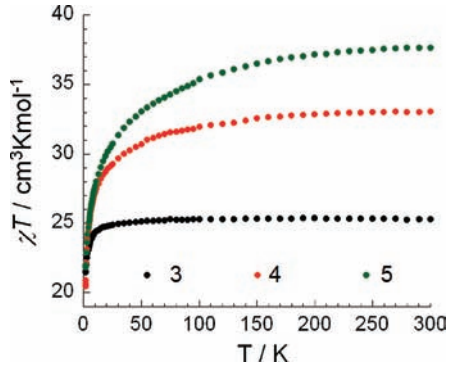

Figure 4. Temperature dependence χT products for **3**−**5** at 1 kOe.

These values are in good agreement with the expected values (24.50 cm^3K/mol for **3**, 32.39 cm^3K/mol for **4** and 37.09 cm^3K/mol for **5**) for two Fe(III) ions ($S = 5/2$, $g = 2$, $C = 4.375$ cm^3K/mol) and two lanthanide(III) ions (Ln = Gd(III); $S = 7/2$, $L = 0$, $g = 2$, $^8S_{7/2}$, $C = 7.88$ cm^3K/mol, Ln = Tb(III); $S = 3$, $L = 3$, $g = 3/2$, $^7F_6$, $C = 11.82$ cm^3K/mol and Ln = Dy(III); $S = 5/2$, $L = 5$, $g = 4/3$, $^6H_{15/2}$, $C = 14.17$ cm^3K/mol).[51] Upon decreasing the temperature, the χT products continuously decrease until 21.53, 20.48, and 21.85 cm^3 K/mol at 1.8 K for compounds **3**−**5**, respectively, indicating the presence of weak intramolecular antiferromagnetic interactions. From a structural point of view, the magnetic interaction between the paramagnetic centers mainly originates from the pairs of lanthanide ions. The interaction of Fe−Ln is likely to be very weak or negligible. The χT product of compound **3** as a function of temperature is almost temperature independent above 30 K, indicating paramagnetic behavior in the temperature range of 30 to 300 K and weakly antiferromagnetic interactions between Gd−Gd below 30 K, which is likely to be the case for the Tb−Tb and Dy−Dy congeners **4** and **5**.

The field dependence of the magnetization at low temperatures shows that the magnetization smoothly increases with the applied dc field (Supporting Information, Figure S1). At 70 kOe, it reaches values of 23.8, 19.8, and 17.8 μ_B for compounds **3**−**5**, respectively. The magnetization of 23.8 μB in **3** is in good agreement with the expected value of 24.0 μB for two Gd(III) (7.0 μB) and two Fe(III) (5.0 μB) ions which are weakly antiferromagnetically coupled. There is no clear saturation for all three compounds, suggesting the presence of magnetic anisotropy and/or the population of low-lying excited states. The magnetic relaxations of compounds **3**−**5** were investigated using ac susceptibility measurements under zero dc field; no out-of-phase signal above 1.8 K and no frequency dependence of the in-phase component was detected.

Mössbauer Spectra of Compounds 1 and 5. Mössbauer spectra of complex **5** are shown in Figure 5. At 3, 30, and 80 K the Mössbauer spectra of compound **5** show a strongly asymmetric high-spin quadrupole doublet with isomer shift of δ = 0.43−0.58 mm/s (relative to α-iron) and

dx.doi.org/10.1021/ic2018264 | *Inorg. Chem.* 2011, 50, 12697−12704

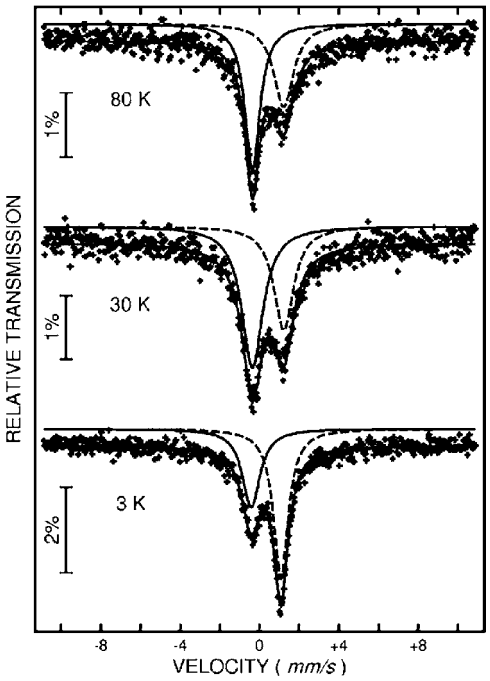

Figure 5. ^{57}Fe Mössbauer spectra of compound **5** at indicated temperatures.

quadrupole splitting of 1.50−1.61 mm/s, which is typical for Fe(III) ions in high spin state. According to the X-ray structure, two quadrupole-split doublets are expected in the Mössbauer spectra. Although one Fe atom is in an octahedral and the other one in a square pyramidal environment it seems that the distortion of the electron cloud around both iron ions is comparable and has a very similar lattice contribution to the electric field gradient (EFG).

Initial fitting attempts were carried out using asymmetric doublets. These afforded only mediocre fits. High quality fits were obtained when the areas of the two peaks of each doublet were fitted separately and the line widths for the obtained singlets were constrained to be equal, although even without constraining the values these were very similar (see Supporting Information, Table S1). An increase in the isomer shift upon cooling is expected due to the second-order Doppler effect.[52] However, in the case of compound **5** we observed a reversed behavior. In general, the temperature dependence of both isomer shift and quadrupole splitting between 3 and 80 K is anomalous. The magnitudes of both of these quantities increase with increasing temperature, contrary to the expected decrease. In principle, it is possible for the electric quadrupole splitting to increase with increasing temperature depending upon the temperature dependence of certain structural parameters, but it is difficult to rationalize the increase in the isomer shift with temperature in the absence of qualitative changes in the electronic structure of the iron ions. We can interpret the temperature dependence of isomer shift as indicating a decrease in the electron density with temperature at the nuclei albeit that it is difficult to see any reason for this. A possible rationalization arises from the fact that it is easy to observe that the Mössbauer spectrum of complex **5** exhibits reversed asymmetry at liquid helium temperature in comparison with the spectra of this complex at 30 and 80 K. This feature is difficult to assign an unambiguous explanation. At first sight, it might suggest a change in sign of the V_{zz} component of the EFG tensors from positive to negative values, but the physical reason for such a temperature dependence is problematical. On the other hand, if we assume that the V_{zz} direction is strongly sensitive to the covalency term of the lattice contribution, this temperature dependence of the asymmetry could be possible, although it is not clear which iron center is more sensitive to this effect. Attempts were made to fit the spectra with two doublets, but in addition to the low quality fits, such attempts gave reasonable spectra only when both doublets exhibit reverse asymmetry. Another attempt at fitting used one symmetric and one asymmetric doublet. Although the parameters for the symmetric doublet were reasonable, those for the asymmetric one were not realistic. A similar strong reverse asymmetry was previously observed for Fe(III) spin crossover compounds[53] and it is reasonable that the signs of V_{zz} are opposite for the low- and high-spin electronic states of the same molecule because of the completely different origins of the EFG tensors. For the low-spin electronic state the EFG tensor results primarily from the asymmetric contribution of valence electrons. In the high-spin case, the valence EFG contribution is negligible and the EFG originates largely in the lattice charges that surround the ^{57}Fe nucleus. Here it must be borne in mind that the line-width values obtained at 30 K should be between the values obtained at 3 and 80 K, but here they are much larger. It thus seems that there could be some lattice transformations which influence not only the V_{zz} direction and, respectively, asymmetry of the peaks, but also isomer shift values. A further possibility is that there is anisotropy of the recoil-free fraction (Goldanskii−Karyagin effect).[54] This possibility arises if the Mössbauer atom is not in a site of cubic symmetry. The Goldanski−Karyagin effect leads to a change of relative peak areas of the two components of a doublet as a function of temperature. With a change in temperature, the line widths of the component lines of a doublet remain unchanged while the areas change. The asymmetry is decreased at low temperature. Upon heating, the accelerated vibrations should cause an increase of the recoil-free fraction anisotropy, and hence of the asymmetry. In the case of compound **5**, we expect to observe a symmetric doublet somewhere between 3 and 30 K. Therefore, we can conclude that in case of compound **5** the possible source of asymmetry in the Mössbauer spectra is anisotropy of the recoil-free fraction (Goldanskii−Karyagin effect) accompanied by the reverse asymmetry.

The Mössbauer spectra for the iron/yttrium complex **1** appear analogous to complex **5** (Supporting Information, Figure S2) apart from the presence of a small and broad magnetic inset at 3 K. The asymmetric anisotropy is also similar to that of compound **5**, which means that the Fe−Fe interactions in compound **5** are not affected by the paramagnetic Dy ions. The Fe−Dy distances are too large and any exchange through the bridging ligands is too weak.

SUMMARY

In summary, a series of iron and rare earth element containing coordination polymers have been successfully prepared using trivalent rare earth nitrates and iron(III) chloride along with the salen ligand H_4L reactions. The novel iron-rare earth element compounds, $\{[Ln_2(FeLCl)_2(NO_3)_2(DMF)_5]\cdot(DMF)_4\}_n$ (Ln = Y, Eu, Gd, Tb, Dy), are polymeric microporous materials. The polymers consist of iron-salen-based moieties having carboxylate linkers connected to rare earth atoms to form a 1D chain structure. The magnetic studies show compounds **3**−**5** exhibit

dx.doi.org/10.1021/ic2018264 | Inorg. Chem. 2011, 50, 12697−12704

weak intramolecular antiferromagnetic interactions. The Mössbauer spectra of compound **5** show strongly asymmetric quadrupole doublets with isomer shift and quadrupole splitting values typical for Fe(III) ions in high spin state. At low temperatures a strong reversed asymmetry was observed which has been presumed to be due to the sign changing of the V_{zz} component of the EFG tensors. Additionally, an anomalous temperature dependence of both isomer shift and quadrupole splitting has been observed.

■ ASSOCIATED CONTENT

Supporting Information

X-ray crystallographic files in CIF format for the structure determinations of **1**−**5** and additional information about the magnetic measurements and the Mössbauer spectra are available free of charge via the Internet at http://pubs.acs.org.

■ AUTHOR INFORMATION

Corresponding Author

*E-mail: roesky@kit.edu; annie.powell@kit.edu.

■ ACKNOWLEDGMENTS

This work was supported by the DFG Center for Functional Nanostructures (CFN).

■ REFERENCES

(1) Robson, R. *J. Chem. Soc., Dalton Trans.* **2000**, 3735−3744.
(2) Robson, R. *Dalton Trans.* **2008**, 5113−5131.
(3) Hoskins, B. F.; Robson, R. *J. Am. Chem. Soc.* **1989**, *111*, 5962−5964.
(4) Hoskins, B. F.; Robson, R. *J. Am. Chem. Soc.* **1990**, *112*, 1546−1554.
(5) Eddaoudi, M.; Kim, J.; Rosi, N.; Vodak, D.; Wachter, J.; O'Keeffe, M.; Yaghi, O. M. *Science* **2002**, *295*, 469−472.
(6) Chae, H. K.; Siberio-Perez, D. Y.; Kim, J.; Go, Y.; Eddaoudi, M.; Matzger, A. J.; O'Keeffe, M.; Yaghi, O. M. *Nature* **2004**, *427*, 523−527.
(7) Oh, M.; Mirkin, C. A. *Nature* **2005**, *438*, 651−654.
(8) Spokoyny, A. M.; Kim, D.; Sumrein, A.; Mirkin, C. A. *Chem. Soc. Rev.* **2009**, *38*, 1218−1227.
(9) Yaghi, O. M.; O'Keeffe, M.; Ockwig, N. W.; Chae, H. K.; Eddaoudi, M.; Kim, J. *Nature* **2003**, *423*, 705−714.
(10) Tranchemontagne, D. J.; Mendoza-Cortes, J. L.; O'Keeffe, M.; Yaghi, O. M. *Chem. Soc. Rev.* **2009**, *38*, 1257−1283.
(11) Maspoch, D.; Ruiz-Molina, D.; Veciana, J. *Chem. Soc. Rev.* **2007**, *36*, 770−818.
(12) Suh, M. P.; Cheon, Y. E.; Lee, E. Y. *Coord. Chem. Rev.* **2008**, *252*, 1007−1026.
(13) Dinca, M.; Long, J. R. *Angew. Chem., Int. Ed.* **2008**, *47*, 6766−6779.
(14) Lee, J.; Farha, O. K.; Roberts, J.; Scheidt, K. A.; Nguyen, S. T.; Hupp, J. T. *Chem. Soc. Rev.* **2009**, *38*, 1450−1459.
(15) Qiu, S.; Zhu, G. *Coord. Chem. Rev.* **2009**, *253*, 2891−2911.
(16) Andruh, M.; Costes, J.-P.; Diaz, C.; Gao, S. *Inorg. Chem.* **2009**, *48*, 3342−3359.
(17) Zhang, X.-M.; Hao, Z.-M.; Zhang, W.-X.; Chen, X.-M. *Angew. Chem., Int. Ed.* **2007**, *46*, 3456−3459.
(18) Allendorf, M. D.; Bauer, C. A.; Bhakta, R. K.; Houk, R. J. T. *Chem. Soc. Rev.* **2009**, *38*, 1330−1352.
(19) Li, Z.; Zhu, G.; Guo, X.; Zhao, X.; Jin, Z.; Qiu, S. *Inorg. Chem.* **2007**, *46*, 5174−5178.
(20) Fang, Q.-R.; Zhu, G.-S.; Xue, M.; Zhang, Q.-L.; Sun, J.-Y.; Guo, X.-D.; Qiu, S.-L.; Xu, S.-T.; Wang, P.; Wang, D.-J.; Wei, Y. *Chem.—Eur. J.* **2006**, *12*, 3754−3758.
(21) Kim, J.; Chen, B.; Reineke, T. M.; Li, H.; Eddaoudi, M.; Moler, D. B.; O'Keeffe, M.; Yaghi, O. M. *J. Am. Chem. Soc.* **2001**, *123*, 8239−8247.
(22) Luo, F.; Batten, S. R. *Dalton Trans.* **2010**, *39*, 4485−4488.
(23) Long, D.-L.; Blake, A. J.; Champness, N. R.; Wilson, C.; Schröder, M. *J. Am. Chem. Soc.* **2001**, *123*, 3401−3402.
(24) Zheng, S.-R.; Cai, S.-L.; Yang, Q.-Y.; Xiao, T.-T.; Fan, J.; Zhang, W.-G. *Inorg. Chem. Commun.* **2011**, *14*, 826−830.
(25) Yin, P.-X.; Li, Z.-J.; Zhang, J.; Zhang, L.; Lin, Q.-P.; Qin, Y.-Y.; Yao, Y.-G. *CrystEngComm* **2009**, *11*, 2734−2738.
(26) Li, Z.; Zhu, G.; Guo, X.; Zhao, X.; Jin, Z.; Qiu, S. *Inorg. Chem.* **2007**, *46*, 5174−5178.
(27) Guo, X.; Zhu, G.; Li, Z.; Chen, Y.; Li, X.; Qiu, S. *Inorg. Chem.* **2006**, *45*, 4065−4070.
(28) Oh, M.; Mirkin, C. A. *Angew. Chem., Int. Ed.* **2006**, *45*, 5492−5494.
(29) Liu, X. *Angew. Chem., Int. Ed.* **2009**, *48*, 3018−3021.
(30) Hobday, M. D.; Smith, T. D. *Coord. Chem. Rev.* **1973**, *9*, 311−337.
(31) Heo, J.; Jeon, Y.-M.; Mirkin, C. A. *J. Am. Chem. Soc.* **2007**, *129*, 7712−7713.
(32) Kitaura, R.; Onoyama, G.; Sakamoto, H.; Matsuda, R.; Noro, S.-i.; Kitagawa, S. *Angew. Chem., Int. Ed.* **2004**, *43*, 2684−2687.
(33) Noro, S.-i.; Kitagawa, S.; Yamashita, M.; Wada, T. *Chem. Commun.* **2002**, 222−223.
(34) Wezenberg, S. J.; Kleij, A. W. *Angew. Chem., Int. Ed.* **2008**, *47*, 2354−2364.
(35) Jung, S.; Oh, M. *Angew. Chem., Int. Ed.* **2008**, *47*, 2049−2051.
(36) Cho, S.-H.; Ma, B.; Nguyen, S. T.; Hupp, J. T.; Albrecht-Schmitt, T. E. *Chem. Commun.* **2006**, 2563−2565.
(37) Jeon, Y.-M.; Heo, J.; Mirkin, C. A. *J. Am. Chem. Soc.* **2007**, *129*, 7480−7481.
(38) Poddar, S. N. *Z. Anorg. Allg. Chem.* **1963**, *322*, 326−336.
(39) Bhunia, A.; Roesky, P. W.; Lan, Y.; Kostakis, G. E.; Powell, A. K. *Inorg. Chem.* **2009**, *48*, 10483−10485.
(40) Roesky, P. W.; Bhunia, A.; Lan, Y.; Powell, A. K.; Kureti, S. *Chem. Commun.* **2011**, *47*, 2035−2037.
(41) Sheldrick, G. M. *Acta Crystallogr., Sect. A* **2008**, *64*, 112−122.
(42) Written by Brand, R. A. University-GH-Duisburg and distributed by Wissel GmbH (Starnberg, Germany).
(43) Johnson, S. L.; Rumon, K. A. *J. Phys. Chem.* **1965**, *69*, 74−86.
(44) Deacon, G. B.; Phillips, R. J. *Coord. Chem. Rev.* **1980**, *33*, 227−250.
(45) Nakamoto, K. *Infrared and Raman Spectra of Inorganic and Coordination Compounds*, 5 ed.; John Wiley & Sons: New York, 1997; Vol. *B*.
(46) Yang, Y.-Y.; Wong, W.-T. *Chem. Commun.* **2002**, 2716−2717.
(47) Guo, X.; Zhu, G.; Sun, F.; Li, Z.; Zhao, X.; Li, X.; Wang, H.; Qiu, S. *Inorg. Chem.* **2006**, *45*, 2581−2587.
(48) Chen, S.-P.; Ren, Y.-X.; Wang, W.-T.; Gao, S.-L. *Dalton Trans.* **2010**, *39*, 1552−1557.
(49) Hernández-Molina, R.; Mederos, A.; Dominguez, S.; Gili, P.; Ruiz-Pérez, C.; Castiñeiras, A.; Solans, X.; Lloret, F.; Real, J. A. *Inorg. Chem.* **1998**, *37*, 5102−5108.
(50) Wang, X.; Pennington, W. T.; Ankers, D. L.; Fanning, J. C. *Polyhedron* **1992**, *11*, 2253−2264.
(51) Benelli, C.; Gatteschi, D. *Chem. Rev.* **2002**, *102*, 2369−2388.
(52) Greenwood, N. N.; Gibbs, T. C. *Mössbauer Spectroscopy*; Chapman and Hall: New York, 1971.
(53) Timken, M. D.; Abdel-Mawgoud, A. M.; Hendrickson, D. N. *Inorg. Chem.* **1986**, *25*, 160−164.
(54) Goldanskii, V. I.; Gorodinskii, G. M.; Karyagin, S. V.; Korytko, L. A.; Krizhanskii, L. M.; Makarov, E. F.; Khrapov, V. V. *Doklady Akad. Nauk S.S.S.R.* **1962**, *147*, 127−130.